

# Engineering analysis of ground motion records of Chile, 2010 earthquake



**L. Liberatore, L. Sorrentino & D. Liberatore**

*“Sapienza” University of Rome, Department of Structural Engineering and Geotechnics*

## SUMMARY:

The 2010 Maule earthquake ( $M_w$  8.8) is one of the largest earthquake occurred since 1900 in the world. The event is an interplate thrust subduction earthquake, with the epicentre located off shore approximately 335 km SW of Santiago. The estimated rupture is about 150 km wide and extends itself approximately 530 km parallel to the coastline. Given the size of the event and of the affected area, it is of some interest to evaluate the recorded ground motion from an engineering standpoint.

In this work, the accelerograms of the Red Sismológica Nacional (= National Seismological Network), recorded in ten different stations from around Santiago in the north to Concepción to the south are analysed. Different intensity measure and different kinds of spectra are computed and discussed. The shaking proves to be rather severe even far from the epicentre, with recorded demand exceeding code demand within the fault projection.

*Keywords: Ground motion, intensity measures, spectral demand, rocking spectra.*

## 1. INTRODUCTION

The earthquake that struck Central Chile on February 27<sup>th</sup> 2010 is one of the largest earthquakes ever recorded. The Moment Magnitude  $M_w$  was as high as 8.8 and the Seismic Moment  $M_0$  was equal to  $1.8-2.0 \times 10^{22}$  N m. The most affected area was about 54 000 km<sup>2</sup> large (United States Geological Survey, <http://earthquake.usgs.gov/earthquakes/eqinthenews/2010/us2010tfan/>, consulted on May, 2011). The population present in the most struck area is in the order of 2 Mi, but in the whole country 8 Mi people were involved. About 520 casualties have been recorded. The homeless were approximately 800 000.

The event was an interplate thrust subduction earthquake, with the epicentre located off shore in a zone where the Nazca plate is being subducted downward and eastward beneath the South American plate. The earthquake occurred as thrust faulting on the interface between the two plates, with an epicentre off coast of Maule Region at 35.909 °S, 72.733 °W and a focal depth of 35 km (USGS, 2010). The estimated rupture is about 150 km wide and extends itself approximately 530 km parallel to the coastline. Apart from the immediate consequences of the earthquake, the subduction of the Nazca plate resulted in an important tsunami that affected a significant portion of the Chilean coast from Iloca to the north, to Tirua to the south. Wave heights up to 10-12 m, excluding splash values, were reported (EERI, 2010 *and references therein*).

Strong shaking lasted for over a minute in a large area, and extensive damage occurred in different cities. A large number of significant aftershocks, consistent with the high magnitude of the main shock, contributed additional damage. Concerning the observed damage, the macroseismic intensity in the MSK (Medvedev-Sponheuer-Karnik) scale was IX in Low Constitución, VIII in Talca and Cauquenes, VII-VIII in Curicó and Concepción (Astroza *et al.*, 2010). In six localities, within Metropolitan Region and fifth Region, intensities VI-VII were estimated. Finally, intensity VI MKS was reported in five Regions of central Chile. Different aspects related to the earthquake, including an

extensive damage account are reported in Decanini *et al.* (2012).

Given the size of the event and of the affected area, it is of some interest the study of the recorded ground motion from an engineering standpoint. In this work, the accelerograms of the RSN have been studied. The signals have been recorded in ten different stations, whose location is shown in Figure 2.1. Different intensity measures have been determined, and displacement, force, energy and rocking spectra have been calculated and discussed. The results have been compared with international records and with Chilean code values.

## 2. STRONG GROUND MOTION

Strong ground motion records have been posted on line by the Red Sismológica Nacional (= National Seismological Network, RSN, [www.sismologia.cl](http://www.sismologia.cl), accessed on February 24, 2011). The Red de Acelerógrafos del Departamento de Ingeniería Civil de la Universidad de Chile (= Accelerographs Network of the Department of Civil Engineering of the University of Chile, RENADIC) also recorded the ground motion. The records, which are not available, have been analysed by Boroschek *et al.* (2010a, 2010b).

In this work, the accelerograms of the RSN, recorded in ten different stations (Table 2.1) have been considered. The accelerograms have been processed by means of a standard software package, using a linear baseline correction and a 4<sup>th</sup> order Butterworth pass-band filter, between 0.1 and 25 Hz.

The location of the ten stations of RSN is presented in Figure 2.1, together with the position of the epicentre and the surface projection of the fault rupture.

Since no geotechnical site classification is available, a tentative classification is made based on the PGA/PGV ratio, according to what proposed by Decanini *et al.* (1999). The soil type is reported in Table 2.1, where soil S1 includes rocks (shear wave velocity  $V_s > 700$  m/s) and stiff deposits ( $400 < V_s < 700$  m/s) with depth  $< 50$  m, soil S2 consists of stiff deposits ( $400 < V_s < 700$  m/s) with depth  $> 50$  m and intermediate soil ( $100 < V_s < 400$  m/s) and soil S3 consists of soft soils ( $V_s < 100$  m/s). The two components of the ground motion do not lead always to the same classification. In such cases, the assessment can be that of stiff-intermediate (S1-S2) or intermediate-soft (S2-S3) soil condition. Apparently most stations are on stiff or intermediate soils, and no case of a station that is definitely on soft soil has been found.

**Table 2.1.** Records and location of stations of the Red Sismológica Nacional.

No.	Record	Station	Lat °. mil	Lon °. mil	Soil type <sup>(1)</sup>	$d_e^{(2)}$ km	$d_p^{(2)}$ km	$d_f^{(2)}$ km
1	ANTU	Fac. de Ciencias Agronomicas, Santiago	-33.569	-70.634	S1-S2	306	90	35
2	CCSP	Colegio San Pedro, Concepción	-36.844	-73.109	S1	113	43	0
3	CLCH	Departamento de Astronomía, Cerro Calan - Las Condes, Santiago	-33.396	-70.537	S2-S3	326	98	53
4	CSCH	Teatro Municipal, Casablanca	-33.321	-71.411	S1-S2	294	65	26
5	LACH	Colegio Las Americas, Santiago	-33.452	-70.531	S2	322	97	49
6	MELP	Compañía de Bomberos, Melipilla	-33.687	-71.214	S1	268	66	0
7	OLMU	Casa particular, Olmué	-32.994	-71.173	S1	335	91	66
8	ROC1	Recinto del Servicio Hidrográfico y Oceanográfico en Cerro El Roble	-32.976	-71.016	S2-S3	342	100	73
9	SJCH	Municipalidad, San José de Maipo	-33.640	-70.350	S1-S2	317	101	57
10	STL	Cerro Santa Lucia, Santiago	-33.440	-70.643	S2-S3	317	94	43

<sup>(1)</sup> Soil type classification is based on PGA/PGV ratios according to what proposed by Decanini *et al.* (1999).

<sup>(2)</sup>  $d_e$  = epicentral distance;  $d_p$  = closest distance to fault plane;  $d_f$  = closest distance to surface projection of the fault rupture.



**Figure 2.1.** Epicentre, surface projection of the fault rupture (reworked after USGS, 2010) and RSN stations.

## 2.1. Intensity measures

The values obtained for classical intensity measures (IMs) for the records of the Chile earthquake are presented in Table 2.2. The references containing the definitions of the considered IMs are recalled at the foot of the table. They are all model-free measures, i.e. they are directly computed from the accelerogram and they are not referred to a specific oscillator.

Surprisingly, maximum values (bolded in Table 2.2) of almost all peak measures were not recorded in Concepción (CCSP), although they are still larger in Concepción than in most of the other stations. This is the case of peak ground acceleration (PGA), velocity (PGV) and displacement (PGD) and effective design acceleration (EDA). Moreover, the records in Concepción are usually the most severe when the entire time history is considered, as in the case of Arias Intensity ( $I_{Arias}$ ), Characteristic Intensity ( $I_c$ ), Specific Energy Density (SED) and Cumulative Absolute Velocity (CAV). This means that, as expected, the number of severe cycles is larger near the causative fault. Nonetheless, it has to be emphasised that durations, even Uniform ( $D_U$ ) and Bracketed ( $D_B$ ) have been rather long in all the stations.

In order to establish a comparison, for each record of the Chilean event, an International strong motion record has been considered. The International records have been selected assuming similar soil conditions and distances from the surface projection of the fault rupture. When more than one record was available, the one with the largest PGA has been chosen. However, the magnitude of the International earthquakes considered is much smaller than that of the Chile event, ranging from 5.6 to 7.6 ( $M_S$ ). Records have been selected from the PEER database (<http://peer.berkeley.edu/smcat/>), except for two Italian records, retrieved from ITACA database (<http://itaca.mi.ingv.it/ItacaNet/>). Details on these events and on the selected records are reported in Sorrentino *et al.* (2012).

The comparison between the IMs evaluated for the two sets of records (Table 2.3) shows that the selected International records are less severe in terms of peak IMs, in average by a factor of about 2.

The same applies for acceleration-related and duration measures. This is due to the magnitude difference in the far field but not close to the causative fault, where the strong-motion parameters become less dependent on magnitude (Bozorgnia and Campbell, 2004). Moreover, the longer durations of RSN signals involve much larger Arias and Characteristic Intensities, as well as Cumulative Absolute Velocity and Specific Energy Density. This contributes to explain the damage level observed in structures suffering cycle repetitions.

**Table 2.2.** Intensity measures of the RSN records; maximum values are bold face.

Record	Comp.	PGA	PGV	PGD	EDA	IV	$I_{Arias}$	$I_c$	SED	CAV	$D_U$	$D_B$	$D_S$
		g	cm/s	cm	g	cm	m/s	$\sqrt{(g^3/s)}$	cm <sup>2</sup> /s	cm/s	s	s	s
ANTU	E	0.279	23.7	13.1	0.250	33.8	2.1	0.061	1520	2328	42	90	38
	N	0.228	28.3	13.0	0.208	40.7	1.9	0.056	2084	2249	48	116	38
	V	0.162	18.1	11.2	0.134	19.8	1.0	0.035	1093	1786	59	129	49
CCSP	E	0.595	48.5	13.7	0.519	65.9	14.2	0.268	<b>7742</b>	7043	67	144	<b>71</b>
	N	0.659	32.5	9.7	0.597	54.2	<b>17.2</b>	<b>0.310</b>	6250	<b>7838</b>	66	144	66
	V	0.551	24.4	7.5	0.424	23.2	11.1	0.223	2014	6107	61	141	63
CLCH	E	0.208	31.3	11.8	0.205	47.8	1.9	0.057	3197	2335	54	146	40
	N	0.217	24.0	12.2	0.213	45.1	1.7	0.052	3079	2282	53	129	45
	V	0.106	18.7	11.8	0.096	18.9	0.7	0.026	1244	1574	<b>72</b>	<b>154</b>	52
CSCH	E	0.328	27.9	10.5	0.330	41.7	3.8	0.114	2326	2842	43	85	30
	N	0.278	28.7	6.4	0.283	55.5	3.7	0.111	1855	2819	49	88	32
	V	0.236	13.6	8.7	0.200	13.1	1.3	0.050	428	1663	40	87	32
LACH	E	0.222	29.7	10.9	0.212	44.4	3.0	0.084	3013	2908	59	127	39
	N	0.293	34.9	12.3	0.286	46.3	3.8	0.099	4220	3181	51	118	37
	V	0.108	21.0	13.5	0.162	33.9	1.6	0.053	2010	2296	69	139	49
MELP	E	<b>0.741</b>	34.0	12.1	<b>0.669</b>	62.4	12.6	0.279	3325	4936	35	74	32
	N	0.576	23.5	10.3	0.485	37.2	8.8	0.214	1593	4207	38	77	32
	V	0.314	16.3	13.7	0.151	15.1	2.1	0.072	985	2068	37	72	34
OLMU	E	0.252	19.6	6.4	0.236	33.0	1.9	0.068	1101	2018	44	90	32
	N	0.367	29.9	5.3	0.336	50.8	4.0	0.119	2228	2788	38	82	28
	V	0.144	9.8	5.0	0.119	14.8	0.7	0.031	337	1211	44	89	34
ROC1	E	0.133	19.9	10.1	0.137	35.8	0.8	0.030	2334	1585	56	143	39
	N	0.196	20.5	6.9	0.185	36.6	1.6	0.048	1483	2068	50	123	33
	V	0.103	10.7	7.5	0.084	15.8	0.4	0.017	437	1066	51	115	38
SJCH	E	0.486	30.4	9.3	0.440	52.8	7.5	0.170	3343	4403	47	95	39
	N	0.476	<b>50.5</b>	14.7	0.484	<b>93.8</b>	6.6	0.154	5393	4125	45	94	38
	V	0.236	24.6	16.1	0.220	29.7	2.1	0.065	2156	2587	61	118	53
STL	E	0.287	42.6	<b>25.3</b>	0.280	65.6	2.8	0.082	4413	2654	47	106	38
	N	0.246	21.6	20.5	0.219	26.4	2.8	0.082	2353	2795	57	110	41
	V	0.262	40.1	19.8	0.253	42.2	2.5	0.075	2636	2649	53	107	41

PG = Peak Ground, A = acceleration, V = Velocity, D = Displacement, EDA = Effective Design Acceleration (Benjamin, 1988), IV = Maximum Incremental Velocity (Anderson & Bertero, 1987),  $I_{Arias}$  = Arias Intensity (Arias, 1970),  $I_c$  = Characteristic Intensity (Park *et al.*, 1985), SED = Specific Energy Density (Kramer, 1996), CAV = Cumulative Absolute Velocity (Cabanas *et al.*, 1991),  $D_U$  = Uniform Duration (Bommer & Martínez-Pereira, 1999),  $D_B$  = Bracketed Duration (Bolt, 1973),  $D_S$  = Significant Duration (Trifunac & Brady, 1975).

**Table 2.3** Comparison between Chilean (RSN) and the considered International accelerograms in terms of peak intensity measures.

Record	PGA	PGV	PGD	EDA	$I_{Arias}$	$I_c$	SED	CAV	$D_U$	$D_B$	$D_S$
	g	cm/s	cm	g	m/s	$\sqrt{(g^3/s)}$	cm <sup>2</sup> /s	cm/s	s	s	s
Chile	0.741	50.5	25.3	0.669	17.2	0.310	7742	7838	66.7	145.8	70.8
Foreign	0.278	36.1	19.8	0.269	0.8	0.039	1164	1065	49.4	74.8	36.8

### 3. DISPLACEMENT, FORCE AND ENERGY SPECTRA

Elastic and inelastic spectral demands, in terms of displacement, force and energy have been evaluated for the processed accelerograms of the RSN stations. The pseudo-acceleration spectra (5% damping) of the horizontal components are reported in Figure 3.1, together with the NCh 433 code elastic spectra. The code spectra of seismic zone II (medium seismicity) has been considered for the comparison with the spectra of Santiago accelerograms (ANTU, CLCH, LACH, STL and SJCH) while seismic zone III (high seismicity) has been considered for the other stations, consistently with the seismic zonation.

The soil classification adopted in this study, based on the PGA/PGV ratio, differs from the classification given in the Chilean code, in which four site soil profiles are defined. Therefore, in some cases two code spectra are depicted, according to the soil type matching reported in Table 3.1. The comparison shows that the code spectra generally overestimate the pseudo-acceleration demand, with the exception of the spectra of the stations CCSP and MELP, which are located on the surface projection of the rupture fault, and SJCH, which is located SE of Santiago. Considering the horizontal components of accelerograms recorded by the RENADIC network (Boroschek *at al.*, 2010b), the pseudo acceleration demand (for a 5% critical damping ratio) is not less than about 2.0 g (at periods less than about 0.5 s) in different stations.

The inelastic spectra for constant displacement ductility equal to 2 and 4 have been also computed. The inelastic demand has been calculated considering a 5% damped single-degree-of-freedom system with degrading cyclic behaviour. The reduction of the spectral demand with ductility is remarkable. On average, the reduction of the peak values is equal to 49% and 62% for ductility equal to 2 and 4, respectively.

**Table 3.1** Soil classifications matching.

Station	Soil type (present study)	Chilean code (NCh 433) soil type
CCSP, MELP, OLMU	S1	type I - type II
ANTU, CSCH, SJCH	S1-S2	type II - type III
LACH, CLCH, ROC1, STL	S2-S3	type III

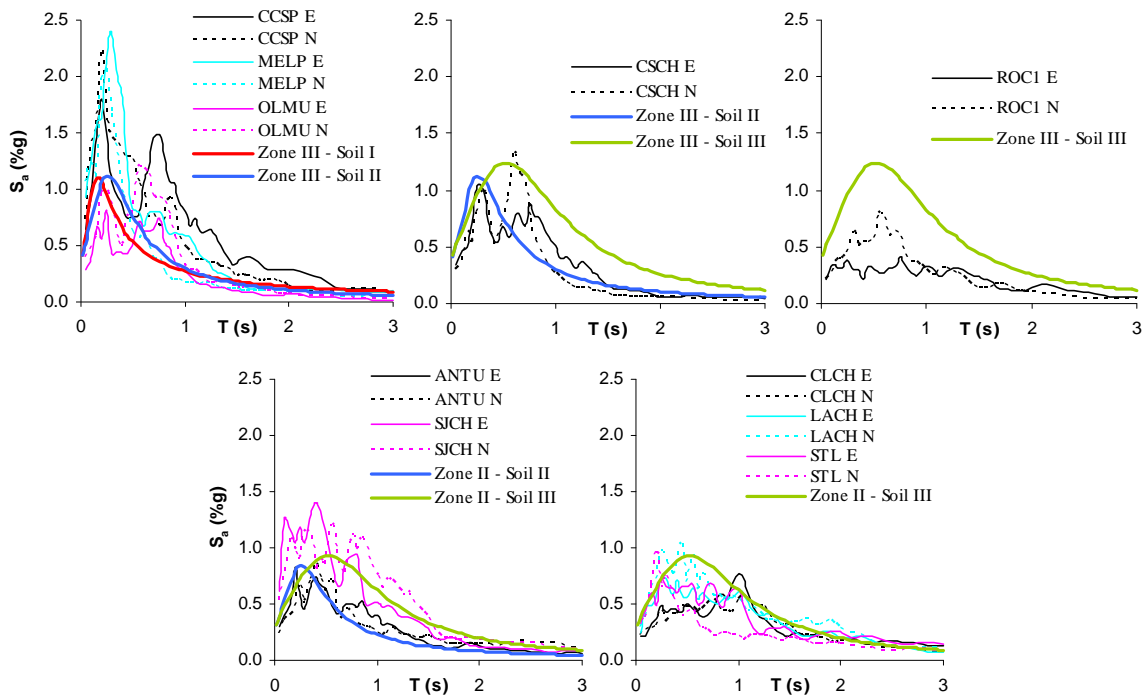


**Figure 3.1.** Pseudo acceleration spectra of the horizontal components and NCh433 elastic code spectra.

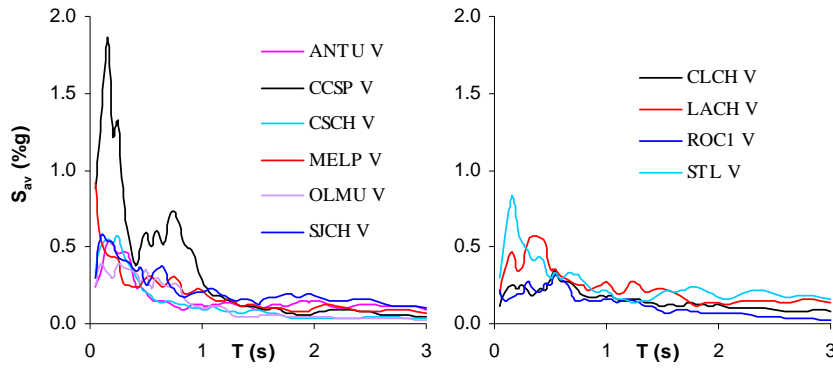


Figure 3.2. Pseudo-acceleration spectra of the vertical component.

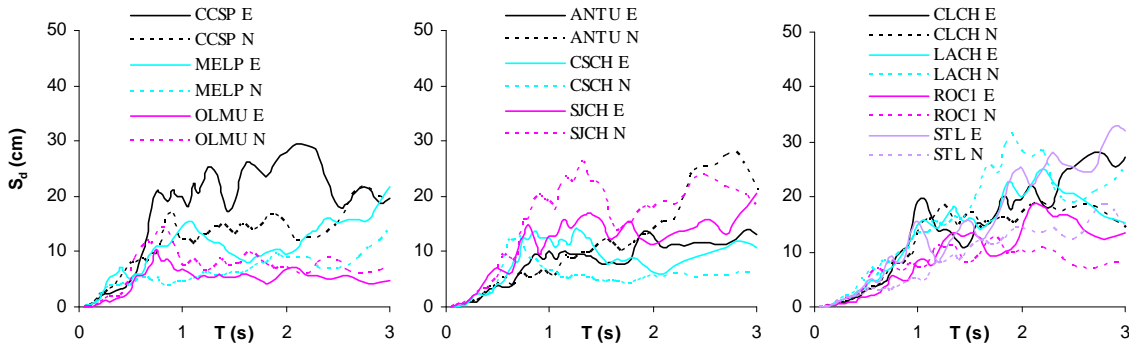


Figure 3.3. Elastic Displacement spectra of the horizontal components.

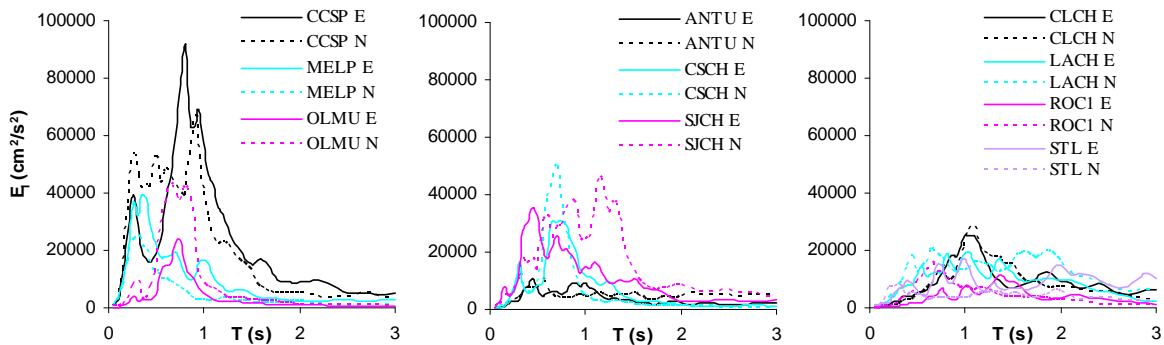


Figure 3.4. Spectra of absolute input energy (for unit mass) of the horizontal components.

In Figure 3.2 the elastic acceleration spectra of the vertical component are shown. The CCSP spectrum shows the highest values, with a peak of 1.86 g (at  $T = 0.15$  s). For the other stations, the peak value of the spectral vertical demand, which occurs at periods not greater than 0.6 s, varies between 0.31 g and 0.91 g. For periods greater than 1.0 s, the demand does not exceed 0.27 g. The NCh 433 code does not suggest an analytical form for the vertical elastic response spectrum; anyway it prescribes to take into account the vertical component of the seismic action in the design of elements vulnerable to this kind of forces (marquises, balconies, etc.). In these cases, a vertical force equal to the dead loads plus the live loads, both multiplied by 1.3, must be considered.

The elastic displacement spectra of the horizontal components are reported in Figure 3.3. The displacement demand in the period range between 0 and 3 s does not exceed 33 cm. The maximum displacement demand occurs at the STL station, which is located more than 40 km away from the fault, but on an intermediate-soft soil. The combination of distance from the fault and soil condition turned out to be important for the evaluation of spectral displacements. For instance, CCSP spectra (stiff soil, near field) are similar to LACH spectra (intermediate-soft soil, far field). Finally, the

comparison with the displacement design spectra suggested by Decanini *et al.* (2003) has shown a somewhat good agreement (Sorrentino *et al.*, 2012).

The absolute input energy for unit mass ( $E_I$ ) is shown in Figure 3.4 for the horizontal components of the motion. Peak values, which occur in the range of periods 0.30-1.35 s, are less than about 50 000  $\text{cm}^2/\text{s}^2$ , with the exception of CCSP spectra, showing a maximum value of about 91 000  $\text{cm}^2/\text{s}^2$ . Peak values are attained at periods that are greater than those at which the maximum acceleration demand occurs, with differences between 0.10 s and 0.75 s.

#### 4. ROCKING SPECTRA

Rocking spectra have been computed for the horizontal accelerograms of the RSN. A rocking spectrum is a plot of the maximum absolute rotation (Makris & Konstantinidis, 2003) sustained by a rigid rocking body (Housner, 1963) of a given frequency parameter  $p$  (related to its mass and shape). The energy damping is related to the height/thickness ratio (Housner, 1963). The rocking body can be assumed to be representative of the behaviour of equipments, free standing walls and slender isolated structures. It is interesting to recall that the seminal paper by Housner (1963) was actually inspired by the performance of water tanks in the Great Chile 1960 earthquake.

In this study, the following ranges of values have been considered:  $2\pi/p = 0-6$  s, corresponding to homogeneous parallelepiped bodies up to 18 m tall;  $h/b = 6-12$  (Figure 4.1). Such figures can be considered typical of both architectural artefacts, such as boundary walls, parapets, obelisks, and of industrial equipment.

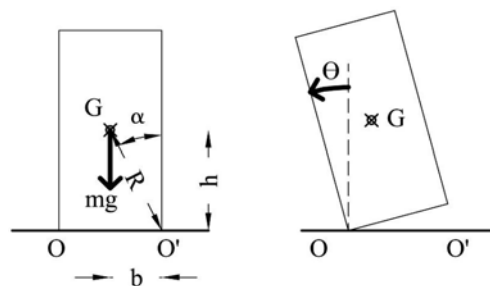


**Figure 4.1.** Parameters describing the Housner model of a rocking rigid body and its displacement.

In order to take into account the scatter of the response, for each pair of  $p$  and  $h/b$  values, 25 time histories have been computed (Sorrentino *et al.*, 2008). These have been obtained by multiplying each accelerogram for 5 amplitude and 5 period scale factors. The scale factors belong to a normal distribution having unity mean and 3% coefficient of variation. Because the problem is unbounded, i.e. the rotation of an overturned body increases without limit, the response has been represented in terms of median maximum absolute normalised rotation,  $Me(\max(|\theta|/\alpha))$ .

Since the behaviour of the oscillator is non-linear elastic, the duration of the excitation is not a significant parameter. However, the physical object resembling to a rocking rigid body may suffer damage due to repeated impact. This can be the case especially of adobe buildings, even if no crumbling of the cross section takes place, as observed elsewhere (Meyer *et al.*, 2007).

Rocking spectra are presented in Figure 4.2. As expected, with limited exceptions, the smaller the height/thickness ratio the smaller the rotation. Moreover, the so called “scale effect” (Housner, 1963) is registered also in this occasion. As a matter of fact, the smaller the frequency parameter  $p$  (i.e. the larger the body) the smaller the rotation. As explained in (Sorrentino *et al.*, 2006) such behaviour is more evident for large amplitude accelerograms (CCSP, MELP, SJCH), whose plots show an abrupt decrease of the median rotation for a small decrease of  $p$  (and thus a small increase in size). The role of  $h/b$  ratio is more marked in low amplitude signals (CLCH, ROC1), which are not able to trigger large amplitude motion in the case of squat bodies.

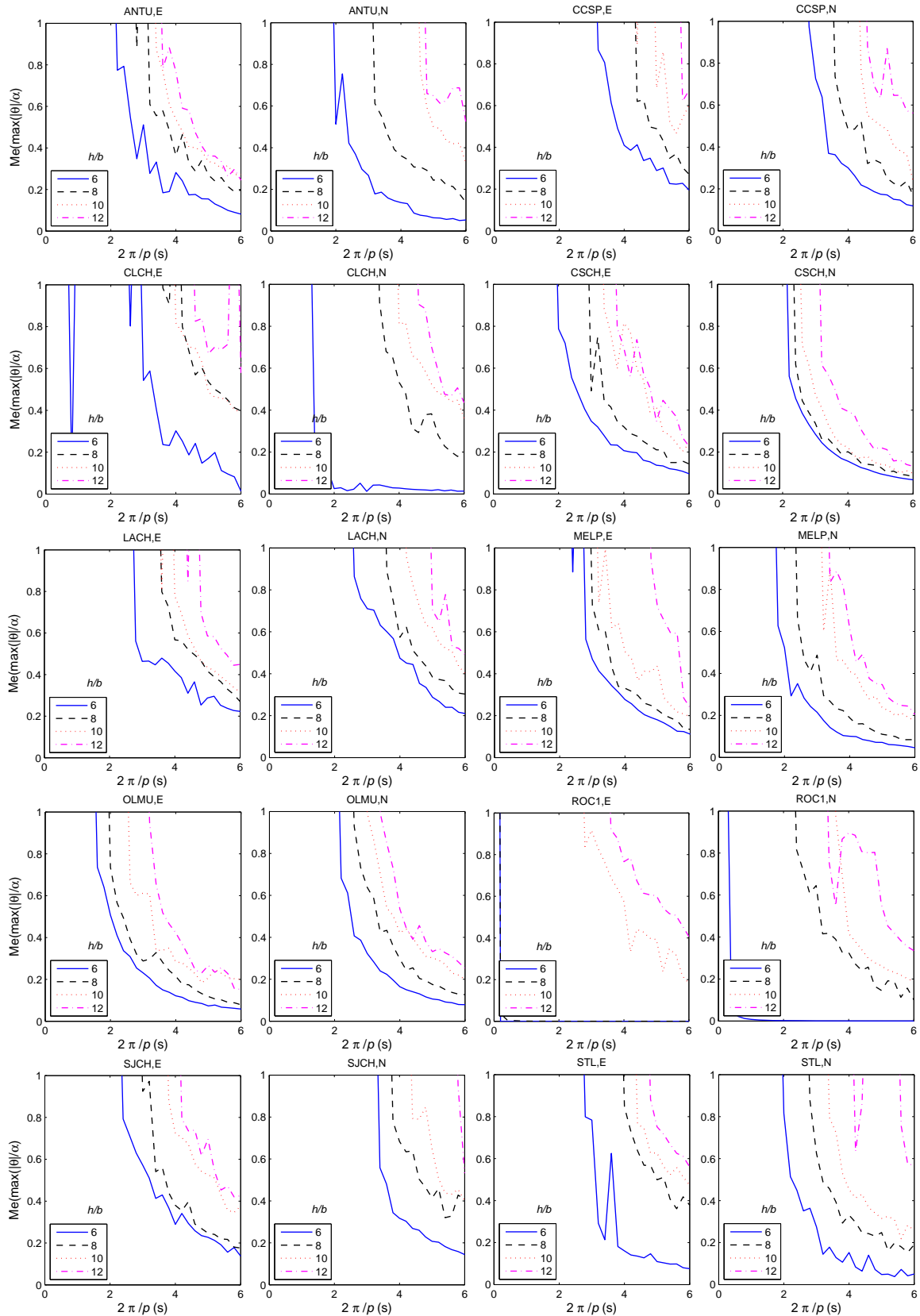


**Figure 4.2.** Rocking spectra for RSN horizontal accelerograms.

The cumulative frequency of overturnings, i.e., the number of overturnings divided by the number of time histories for all the  $h/b$  ratios is reported in Table 4.1. It is clear that, although the EW component of the CCSP station is the most severe accelerogram, all the records are able to cause a significant

number of collapses. This is the case even rather far away from the focus and the fault. Since existing unreinforced masonry buildings frequently suffer local collapse mechanisms, and these are usually rocking mechanisms, such result can contribute to explain the significant damage observed in masonry structures even in Santiago.

**Table 4.1** Cumulative frequency of overturning of the rocking spectra (%).

Station	ANTU	CCSP	CLCH	CSCH	LACH	MELP	OLMU	ROC1	SJCH	STL
E component	48	72	59	48	56	54	36	27	55	64
N component	56	61	53	40	63	42	45	40	69	52

The same spectra have been computed for the foreign records that were selected for comparison purposes. The comparison shows that Chilean records are much more severe. Comparing the cumulative frequency of overturnings for the considered International records to those of the Chilean accelerograms, it can be noted that whereas international records have an average cumulative frequency of overturning equal to 21%, Chilean records have an average value of the same parameter equal to 52%. Moreover, the scatter of the response is much more significant.

## 5. SUMMARY AND CONCLUSIONS

In this study, the accelerograms recorded during the Maule earthquake have been analysed. The accelerograms of the RSN stations, which are located mainly in Santiago Region and in the V Region, have been processed in order to calculate intensity measures and response (acceleration, displacement, energy, rocking) spectra. Chilean accelerograms have been also compared to other International accelerograms, recorded for similar soil condition and distance from the fault plane. The main conclusions can be summarized as follows:

- Maximum intensity measures based on peak values (e.g., PGA, PGV, PGD) do not occur in Concepción, but further away from the fault. Anyway, the records in Concepción are usually the most severe when the entire time history is considered, as in the case of Arias Intensity and Cumulative Absolute Velocity, or when spectral values are examined.
- The pseudo-acceleration demand generally does not exceed the NCh 433 elastic spectra, with the exception of the stations located within the surface projection of the fault, whose pseudo-acceleration demand is greater than 2 g. Anyway, considering RENADIC accelerograms, significant spectral amplifications have been observed also in the area of Santiago. Vertical acceleration spectra show largest values (up to 1.8 g) close to the fault. As expected, the inelastic demand is significantly lower than the elastic demand. In fact, for a constant ductility of 2, the maximum spectral accelerations decrease of about 50%.
- The displacement demand does not exceed 33 cm. The NCh 433 displacement spectra (derived from the elastic acceleration spectra) are similar to those of the recorded accelerograms, with the exception of the stations closest to the fault.
- The absolute input energy spectra show a significant difference between the energy demand in Concepción and that evaluated at other stations.
- Rocking spectra have confirmed previous results about the role of the size and the height/thickness ratio of the system. Moreover, they highlight a significant damage potential even rather far away from the fault plane. This can contribute to explain the performance of masonry structures in the area of Santiago. Compared to the considered International records, Chilean accelerograms prove again much more severe.
- Peak intensity measures of Chilean signals are twice those of the considered International records, partly due to the smaller magnitude related to the International records. If intensity measures computed over the entire time history are considered, Chilean accelerograms are from 6 to 15 times more severe. This can account for the damages observed on structures vulnerable to cycle reversals.

## ACKNOWLEDGEMENT

The financial support of the Ministry of the Instruction, University and Research of Italy (MIUR) is gratefully acknowledged. This work has been partially carried out under the program “Dipartimento di Protezione Civile –

Consorzio RELUIS”, signed on 2009-09-24 (n. 823), whose financial support is greatly appreciated. The valuable comments and suggestions of Prof. Luis Decanini are gratefully acknowledged.

## REFERENCES

- Anderson, J. C. and Bertero, V. V. (1987). Uncertainties in Establishing Design Earthquakes. *ASCE Journal of Structural Engineering*, **Vol. 113**, pp. 1709-24.
- Arias, A. (1970). A measure of earthquake intensity. R.J. Hansen (ed). Seismic Design for Nuclear Power Plants: 438-483, Massachusetts Institute of Technology Press, Cambridge, Massachusetts.
- Astroza, M. I., Cabezas, F. M., Moroni, M. O. Y., Massone, L. S., Ruiz, S. T., Parra E., Cordero, F. O. and Mottadelli, S. (2010). Intensidades sísmicas del terremoto del 27 de febrero de 2010, Departamento de Ingeniería Civil, Facultad de Ciencias Físicas y Matemáticas Universidad de Chile, Santiago.
- Benjamin, J. R. (1988). A criterion for determining exceedance of the Operating Basis Earthquake, EPRI Report NP-5930, Electric Power Research Institute, Palo Alto, California.
- Bolt, B. A. (1973). Duration of strong ground motion. *Proceedings 5th World Conference on Earthquake Engineering*, Rome, pp. 1304–1313.
- Bommer, J. J. and Martínez-Pereira, A. (1999). The effective duration of earthquake strong motion. *Journal of Earthquake Engineering*, **Vol. 3**, pp. 127-172.
- Boroschek, R., Soto, P., Leon, R. and Compte, D. (2010a). Terremoto centro sur Chile 27 de Febrero de 2010, Informe Preliminar n. 4. Universidad de Chile, Facultad de Ciencias Físicas y Matemáticas, Departamento de Ingeniería Civil, Informe preliminar. April 2010. <http://www.terremotosuchile.cl/#info>
- Boroschek, R., Soto, P. and Leon, R. (2010b). Registro del terremoto del Maule  $M_W = 8.8$  - 27 de Febrero de 2010, Universidad de Chile, Facultad de Ciencias Físicas y Matemáticas, Departamento de Ingeniería Civil, Informe RENADIC 10/05 Rev.1 Octubre 2010. <http://www.terremotosuchile.cl/#info>
- Bozorgnia, Y. and Campbell, K. W. (2004). Engineering Characterization of Ground Motion. Pp. 5.1-74. Bozorgnia Y., Bertero V. V. *Earthquake Engineering. From Engineering Seismology to Performance-Based Engineering*. Boca Raton – London – New York – Washington: CRC.
- Cabanas, L., Benito, B. and Herraiz, M. (1991). Approach to the measurement of the potential structural damage of earthquake ground motions. *Earthquake Engineering and Structural Dynamics*, **Vol. 26**, pp. 79-92.
- Decanini, L. D. and Mollaioli, F. (1998). Formulation of Elastic Earthquake Input Energy Spectra. *Earthquake Engineering and Structural Dynamics*, **Vol. 27**, pp. 1503-1522.
- Decanini, L., Di Pasquale, G. and Mollaioli, F. (1999). Valutazione del Potenziale Distruttivo della Sequenza Sismica Umbro – Marchigiana. *IX Convegno Nazionale L’Ingegneria Sismica in Italia*, Torino, – in Italian.
- Decanini, L. D., Liberatore, L. and Mollaioli, F. (2003). Characterization of displacement demand for elastic and inelastic SDOF systems. *Soil Dynamics and Earthquake Engineering*, **Vol. 23**, pp. 455-471.
- Decanini, L. D., Liberatore, D., Liberatore, L., Sorrentino, L., Magenes, G. and Penna A. (2012). Report on the Maule (Chile) February 27th, 2010 earthquake, Pavia, IUSS Press.
- EERI (Earthquake Engineering Research Institute) Special Earthquake Report (2010) Learning from Earthquakes. The Mw 8.8 Chile Earthquake of February 27, 2010, <http://www.eqclearinghouse.org/20100227-chile/published-reports>
- Housner, G. W. (1963). The behavior of inverted pendulum structures during earthquakes. *Bulletin of the Seismological Society of America*, **Vol. 53**, pp. 403-417.
- Kramer, S. L. (1996). Geotechnical Earthquake Engineering, Prentice-Hall, Upper Saddle River, New Jersey.
- Makris, N. and Konstantinidis, D. (2003). The rocking spectrum and the limitations of practical design methodologies. *Earthquake Engineering and Structural Dynamics*, **Vol. 32**, pp. 265–289.
- Meyer, P., Ochsendorf, J., Germaine, J. and Kausel, E. (2007). Impact of High-Frequency/Low-Energy Seismic Waves on Unreinforced Masonry. *Earthquake Spectra*, **Vol. 23**, pp. 77-94.
- NCh 433 Of 1972, 1993 and 1996. Diseño Sísmico de Edificios, Instituto Nacional de Normalización, Santiago.
- Park, Y. J., Ang, H. S. and Wen, Y. K. (1985). Seismic damage analysis of reinforced concrete buildings. *ASCE Journal of Structural Engineering*, **Vol. 111**, pp. 740-757.
- Sorrentino, L., Masiani, R., Decanini, L.D. (2006). Overturning of rocking rigid bodies under transient ground motions. *Structural Engineering and Mechanics*, **Vol. 22**, pp. 293-310.
- Sorrentino, L., Kunnath, S., Monti, G. and Scalora, G. (2008). Seismically induced one-sided rocking response of unreinforced masonry façades. *Engineering Structures*, **Vol. 30**, pp. 2140-2153.
- Sorrentino L, Liberatore L, Decanini L. D. (2012). Strong ground motion. Report on the Maule (Chile) February 27<sup>th</sup>, 2010 earthquake, Pavia, IUSS Press.
- Trifunac, M. D. and Brady, A. G. (1975). A study on the duration of strong earthquake ground motion. *Bulletin of the Seismological Society of America*, **Vol. 65**, pp. 581-626.